Chapter 4

Absorption and Desorption Mass Transfer Rates in Non-Reactive Systems

Abstract

Liquid phase mass transfer coefficients have been measured in a controlled environment during gas absorption into a liquid and gas desorption from a liquid in a batch operated stirred tank reactor over a wide range of operating conditions. At identical operating conditions, the mass transfer coefficients for absorption and desorption appears to be the same within the reported experimental uncertainty. The desorption mass transfer coefficients depend, in the same manner as the absorption mass transfer coefficients, on the physico-chemical and the dynamic properties of the system, and can thus be related by the Sherwood, Reynolds, and Schmidt numbers. Desorption mass transfer processes can be further described by the well-known film theory, the penetration theory, the surface renewal theory, etc. in the same manner as absorption mass transfer processes.

4.1 Introduction

Mass transfer is the basis of many (chemical) processes and underlies the various separation processes where one or more components migrate within one phase or from one phase to another and occurs in the net direction of a decreasing chemical potential. The mechanism of mass transfer depends upon the dynamics of the system(s) in which it occurs. Mass can be transferred by two distinct modes of transport, *molecular mass transfer* and *convective mass transfer*. Whenever a mixture contains two or more molecular components of different relative compositions from point to point, an apparent natural process occurs which tends to diminish any inequalities of composition. This macroscopic transport of mass, independent of any convection within the system, is defined as molecular mass transfer. Mass transfer between phases, immiscible mixtures, and partially miscible mixtures is often a result of the moving dynamics of/in the system. This mode of transfer is called convective mass transfer, and depends on both the transport properties and the dynamic characteristics of the migrating component(s). A distinction must be made between two types of convective mass transfer. If a pump, rotor, or a similar device causes a motion resulting in mass transfer, the process is called *forced convection*. If the mass transport is due to density differences, the process is called *free* or *natural convection*. [79, 80]

Gas absorption is undoubtedly the single most important industrial operation of gas purification mass transfer processes and is used in an extensive amount. This process is frequently coupled with a desorber to permit regeneration and recycling of the absorbent.

Traditionally, focus and attention have been given to the improvement of the gas absorber section through better (reactive) absorbent(s), gas-liquid mass transfer characteristics, heat integration, etc. This has been carried out mainly for the improvements of high pressure gas treating processes, such as natural gas. [1, 81] The gas desorber section has lately gained increased focus and attention, in the interest of reducing the energy consumption of gas desorption from a (reactive) absorbent. This is of particular financial interests in the case of the removal of low to medium partial pressure carbon dioxide from gas streams, e.g. flue gases. Still, fundamental aspects of gas desorption characteristics are absent in the open literature. When a gas is desorbed, the concentration of the dissolved gas in the bulk of the liquid is greater than that at the interface. If the total pressure at the interface is sufficiently less than that in the liquid bulk, bubbles will begin to form in the bulk and much of the gas will be released by diffusion to the interface of the bubble. This is a process very different from the absorption process, in which the interfacial area is determined by external factors and not the process itself. When the partial pressure of the gas in the liquid bulk has fallen to a value equal to the total pressure at the interface, bubbling will cease. The desorption process will further continue to the normal interfacial area and be limited by diffusion until equilibrium between the partial pressures in the bulk and the interface is achieved. [81] It is often assumed that the theory and principles for absorption processes are also valid for this diffusion limited desorption process, and that these are symmetrical of each other. In that sense, the mass transfer of a migrating compound between a gas phase and a liquid phase should be equal at identical operating conditions during the absorption and desorption process. This is usually assumed and accepted; however, experimental validation in the open literature is extremely limited. In studies where absorption and desorption mass transfer processes have been studied and compared, the volumetric mass transfer coefficients ($k_l a$) have often been compared to one another and by such not the mass transfer coefficients (k_l). Discrepancies of the volumetric mass transfer coefficients have been observed and reported for absorption and desorption mass transfer processes; although, the interfacial area (a) was not necessarily known or held constant. [82–87] The purpose of the current work is to obtain more fundamental insights of absorption and desorption forced convective mass transfer processes by comparing mass transfer coefficients (k_l) for absorption and desorption processes to one another over a wide range of identical operation conditions.

4.2 Theory and experimental procedure

According to mass transfer theories such as the (two-) film theory, the penetration theory, the surface renewal theory, etc., the mass transfer of a process will depend on the diffusivity, D, and the convective motion (e.g. hydrodynamics) of the compounds involved. The diffusivity is usually related to the mass transfer coefficient, k, by:

$$k \propto D^r \tag{4.1}$$

where r usually varies between 0.5 and 1.0. The relation between the mass transfer coefficient and the motion of the components involved can not be generally correlated, and depends upon geometries, stirrer/pump speed, etc. of the equipment used. Therefore, for a justified comparison of mass transfer in both directions over an interface, the diffusivity D and the convective motion of the compounds involved have to be kept constant. Absorption and desorption measurements have been carried out in a stirred cell at identical temperature, stirrer speed, bulk volumes, solvent concentration, and interfacial area in the present work. Although the comparable measurements were carried out at identical operating conditions, the operating conditions such as the hydrodynamics (stirrer speed and liquid levels), temperatures, and chemical compounds were changed in order to obtain a wide range of comparable measurements.

It is common practice to describe the dependency of the experimentally observed mass transfer coefficients to the molecular diffusivity, viscosity, density, and hydrodynamics of the system by means of a relationship of dimensionless numbers for absorption measurements. [88, 89] The well-known relation relating the Sherwood (Sh) number to the Reynolds (Re) and Schmidt (Sc) numbers applied to a stirred tank is:

$$Sh = c1 + c2Re^{c3}Sc^{c4} \tag{4.2}$$

where:

$$Sh = \frac{k_l d_s}{D} \tag{4.3}$$

$$Re = \frac{d_s^2 \omega \rho}{\mu} \tag{4.4}$$

$$Sc = \frac{\mu}{\rho D} \tag{4.5}$$

The constants $c1$, $c2$, $c3$, and $c4$ in Equation (4.2) are dependent on the type of equipment used, e.g. geometries of the tank, stirrer type/speed, etc. From the results in the present work, it was concluded that the constant $c1$ could be neglected. The exponent $c3$ of the Re number can easily be determined experimentally by variation of the Sh and Re number, i.e. variation of the stirrer speed, and simultaneously keeping the solute/solvent dependent Sc number constant. The coefficient $c2$ and the exponent $c4$ can be determined by using different solutes/solvents at constant Re numbers, i.e. identical hydrodynamic conditions.

The liquid phase mass transfer coefficient, k_l was determined for both physical absorption and desorption with the following systems; carbon dioxide - water, oxygen - water, nitrous oxide - aqueous N-methyldiethanolamine (MDEA), and nitrous oxide - aqueous diisopropanolamine (DIPA). In this way, the solubilities of the gaseous compound in the liquid solution and the viscosities of the liquid solution could be varied over a wide range and thus covering different experimental conditions, i.e. Sc numbers. The diffusivity of the gaseous compounds in the liquid solutions varies with the viscosities of the solution [90], and alters the mass transfer coefficient according to Equation (4.1). A schematic presentation and specifications of the setup used are given in Figure 4.1 and Table 4.1. The reactor consisted of glass and stainless steel metal, was thermostatted to within ±0.1 K, and provided with 2-blade independently controlled stirrers in the gas and the liquid phase at fixed positions inside reactor. Both the reactor and the gas supply vessel were equipped with PT-100 temperature sensors and high precision pressure transducers (Heise Model DXD, range 0 to 2 bara). The maximum stirrer speed at which a visual smooth interface could still be maintained for the type of stirrers used was at about 2.62 revolutions per second (rps). By the use of a high purity single component gas during each measurement, gas phase mass transfer resistance could be neglected. In the case of the carbon dioxide - water system; the reaction rate between carbon dioxide and water and the conversion of carbon dioxide were far to low to enhance the mass transfer rate [91] and thus neglected. The experiments were carried out batchwise with respect to both phases. The

Table 4.1: Dimensions of the experimental setup

Volume of reactor	V	$4.335{\cdot}10^{-3}\mathrm{m}^3$
Volume liquid phase	V_l	2.041 - $2.450{\cdot}10^{-3}\mathrm{m}^3$
Interfacial area	a	$1.772{\cdot}10^{-2}\mathrm{m}^2$
Stirrer revolutions per second (rps)	ω	0.87 - 2.62
Stirrer diameter	d_s	0.10 m
Liquid height in reactor	h	0.121 - 0.140 m

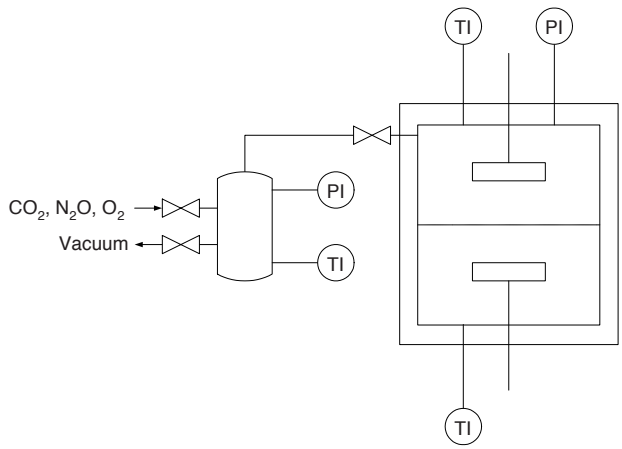

Figure 4.1: Schematic drawing of the experimental setup

transient absorption and desorption rates were thus given by:

$$V_g \frac{\mathrm{d}C_g^b}{\mathrm{d}t} = -k_l a \left(m C_g^b - C_l^b\right) \tag{4.6}$$

where:

$$m = \frac{C_l^i}{C_g^i} \tag{4.7}$$

The superscripts b and i refers to the bulk and interface and m can be regarded as a distribution coefficient. The conservation of mass gives:

$$V_g C_g^0 + V_l C_l^0 = V_g C_g^b + V_l C_l^b \tag{4.8a}$$

$$C_g^\infty = \frac{V_g C_g^0 + V_l C_l^0}{m V_l + V_g} \tag{4.8b}$$

where the superscripts 0 and ∞ refers to the initial and infinite time. Solving Equations (4.6), (4.8a), and (4.8b) with respect to C_g^b and t using the following initial condition:

$$C_g^b = C_g^0 \text{ at } t = 0 \tag{4.9}$$

yields:

$$ln\left[\frac{C_g^b - C_g^\infty}{C_g^0 - C_g^\infty}\right] = -\frac{(m V_l + V_g)\,(k_l a)\,t}{V_g V_l} \tag{4.10}$$

By means of the ideal gas law and Equations (4.7) and (4.10) the mass transfer coefficient, k_l, was calculated from the measured transient pressure change. By plotting the left side of Equation (4.10) versus the time t, the mass transfer coefficient can easily be determined from the slope.

The absorption and desorption experiments were carried out at two temperatures, 298.15 K and 313.15 K, and two liquid levels inside the reactor, 0.121 m and 0.140 m. At the start of the experiment, a known amount of liquid at a known composition was introduced into the reactor and the liquid phase stirrer was set to a specific number of rps. [55,92] The solution was degassed

for a period of time in order to remove any dissolved gases. After equilibration, the gaseous component was introduced to the reactor within a few seconds from the gas supply vessel as shown in Figure 4.1. The reactor pressure decrease was recorded over a period of time until phase equilibrium was reached. The absorption mass transfer coefficient was calculated from the recorded data by the use of Equation (4.10) as aforementioned. The desorption measurement followed directly after the absorption measurement. By such the solution which contained the absorbed gas was used directly for the desorption measurement. The stirrer was kept at the same rps as during the absorption experiment. Vacuum was applied to the gas supply vessel by means of a vacuum pump. The valve between the vessel and the reactor was carefully opened for a very short time, and some of the gaseous component was transferred from the reactor into the gas supply vessel by means of the pressure difference. At the same time, some of the solvent vapor present in the gas phase was transferred along with the gaseous component. The removed solvent vapor was however replaced within a few seconds by the liquid solvent, and any very small change in the concentration of the solvent was neglected. In order to avoid any visual gas bubble formation in the liquid phase, and hence a change of the interfacial area, the pressure decrease had to be less than about 30 mbar for the reactor used. The sudden pressure decrease in the reactor was further succeeded by a slow pressure increase of the gaseous compound from the liquid phase into the gas phase to phase equilibrium. The desorption mass transfer coefficient was calculated from Equation (4.10) as aforementioned. Physical properties such as viscosities, diffusivities, densities, etc. of the solution were assumed to remain constant throughout the measurement. Figure 4.2 shows a typical absorption measurement followed by a typical desorption measurement in Figure 4.3 presented for the convenience of the reader.

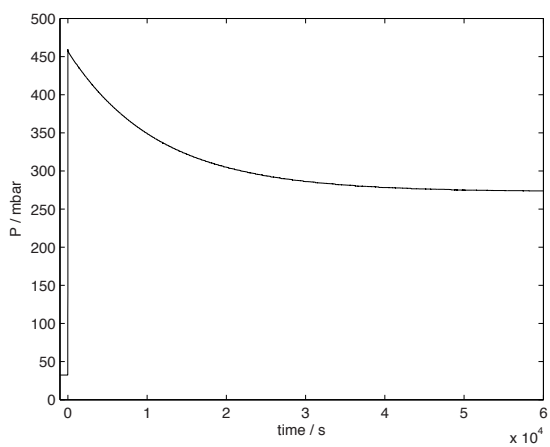

Figure 4.2: Typical absorption measurement

4.3 Results and discussion

The overall results of the liquid phase mass transfer coefficients for absorption and desorption are given in Table 4.2 and as a parity plot in Figure 4.4. The desorption mass transfer coefficients are given with error bars in Figure 4.4 which represents the inaccuracy of the pressure transducer of ± 0.1 mbar. As expected, the mass transfer coefficients are higher at higher temperatures,

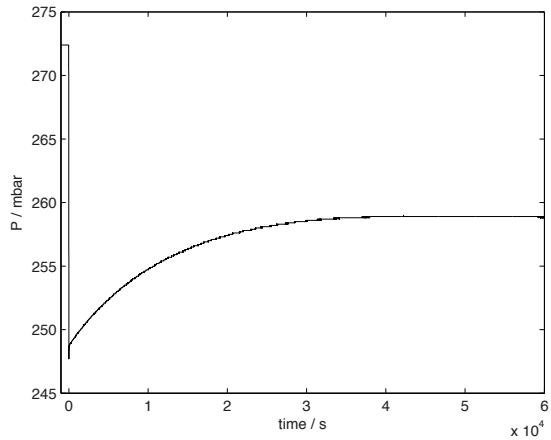

Figure 4.3: Typical desorption measurement

stirrer speeds, and lower liquid levels. The latter is a result of higher mixing at the interface due to the immediate presence of the liquid phase stirrer. The mass transfer coefficients for comparable measurements appears to be the same within the reported experimental uncertainty for absorption and desorption. The largest absolute difference between an absorption and a desorption mass transfer coefficient in the results presented is $0.05{\cdot}10^{-5}$ m·s^{-1}, resulting in a relative difference of 3.94%. The obtained results were further used to study the influence of

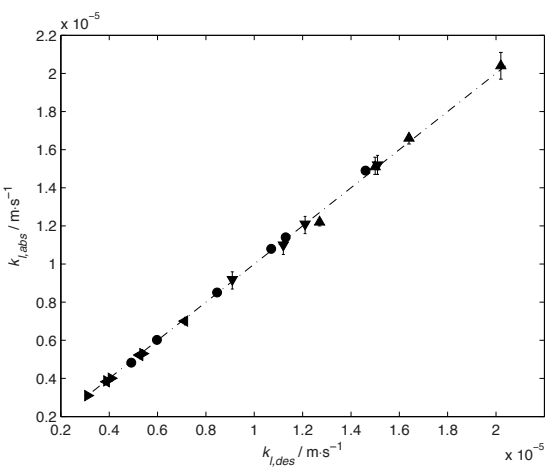

Figure 4.4: Comparison of liquid phase mass transfer coefficients: •, carbon dioxide - water at $T = 298.15$ K; ▲, carbon dioxide - water at $T = 313.15$ K; ▼, oxygen - water at $T = 298.15$ K; ◄, nitrous oxide - 2M aq. MDEA at $T = 298.15$ K; ►, nitrous oxide - 2M aq. DIPA at $T = 298.15$ K.

Table 4.2: Overall results of the liquid phase mass transfer coefficients

Run.	$k_{l,abs}$ / m·s^{-1}	$k_{l,des}$ / m·s^{-1}	abs. dev.	ω / rps.	h / m
carbon dioxide - water at 298.15 K					
1	$6.02{\cdot}10^{-6}$	$5.97{\cdot}10^{-6}$	$-0.05{\cdot}10^{-6}$	0.87	0.121
2	$1.08{\cdot}10^{-5}$	$1.07{\cdot}10^{-5}$	$-0.01{\cdot}10^{-5}$	1.75	0.121
3	$1.49{\cdot}10^{-5}$	$1.46{\cdot}10^{-5}$	$-0.03{\cdot}10^{-5}$	2.62	0.121
4	$4.83{\cdot}10^{-6}$	$4.91{\cdot}10^{-6}$	$0.05{\cdot}10^{-6}$	0.87	0.140
5	$8.51{\cdot}10^{-6}$	$8.46{\cdot}10^{-6}$	$-0.05{\cdot}10^{-6}$	1.75	0.140
6	$1.14{\cdot}10^{-5}$	$1.13{\cdot}10^{-5}$	$-0.01{\cdot}10^{-5}$	2.62	0.140
carbon dioxide - water at 313.15 K					
7	$1.51{\cdot}10^{-5}$	$1.50{\cdot}10^{-5}$	$-0.01{\cdot}10^{-5}$	1.75	0.121
8	$2.04{\cdot}10^{-5}$	$2.02{\cdot}10^{-5}$	$-0.02{\cdot}10^{-5}$	2.62	0.121
9	$1.22{\cdot}10^{-5}$	$1.27{\cdot}10^{-5}$	$0.05{\cdot}10^{-5}$	1.75	0.140
10	$1.66{\cdot}10^{-5}$	$1.64{\cdot}10^{-5}$	$-0.02{\cdot}10^{-5}$	2.62	0.140
oxygen - water at 298.15 K					
11	$1.10{\cdot}10^{-5}$	$1.12{\cdot}10^{-5}$	$0.02{\cdot}10^{-5}$	1.75	0.121
12	$1.52{\cdot}10^{-5}$	$1.51{\cdot}10^{-5}$	$-0.01{\cdot}10^{-5}$	2.62	0.121
13	$9.19{\cdot}10^{-6}$	$9.09{\cdot}10^{-6}$	$-0.10{\cdot}10^{-6}$	1.75	0.140
14	$1.21{\cdot}10^{-5}$	$1.21{\cdot}10^{-5}$	0	2.62	0.140
nitrous oxide - 2M aq. MDEA at 298.15 K					
15	$5.24{\cdot}10^{-6}$	$5.26{\cdot}10^{-6}$	$0.02{\cdot}10^{-6}$	1.75	0.121
16	$7.01{\cdot}10^{-6}$	$7.12{\cdot}10^{-6}$	$0.11{\cdot}10^{-6}$	2.62	0.121
17	$3.83{\cdot}10^{-6}$	$3.88{\cdot}10^{-6}$	$0.05{\cdot}10^{-6}$	1.75	0.140
18	$5.24{\cdot}10^{-6}$	$5.26{\cdot}10^{-6}$	$0.02{\cdot}10^{-6}$	2.62	0.140
nitrous oxide - 2M aq. DIPA at 298.15 K					
19	$4.01{\cdot}10^{-6}$	$4.08{\cdot}10^{-6}$	$0.07{\cdot}10^{-6}$	1.75	0.121
20	$5.30{\cdot}10^{-6}$	$5.39{\cdot}10^{-6}$	$0.09{\cdot}10^{-6}$	2.62	0.121
21	$3.10{\cdot}10^{-6}$	$3.11{\cdot}10^{-6}$	$0.01{\cdot}10^{-6}$	1.75	0.140
22	$3.87{\cdot}10^{-6}$	$3.90{\cdot}10^{-6}$	$0.03{\cdot}10^{-6}$	2.62	0.140

the stirrer speed on the mass transfer coefficients. From Equation (4.2) the following relation can be derived given a constant Sc number:

$$k_l \propto \omega^{c3} \tag{4.11}$$

The results of the system carbon dioxide - water at 298.15 K are presented in Figure 4.5. The mass transfer coefficients show a higher dependency on the stirrer speed when the liquid level in the reactor is low, which is as expected since the stirrer is located closer to the interfacial area resulting in a more pronounced mixing and different hydrodynamics. The dependency of the mass transfer coefficients on the stirrer speed and the liquid levels is the same for both the absorption and the desorption measurements. For the reactor used in the current work $c3$ was found to be 0.694 and 0.583 for the liquid levels of 0.121 m and 0.140 m, respectively. These values were assumed to be independent of the different systems, but dependent on the liquid levels in the reactor. [89] Rearranging Equation (4.2) yields:

$$Sh/Re^{c3} = c2Sc^{c4} \tag{4.12}$$

By applying the values of the constant $c3$ to the respective systems, the dependence of Sh/Re^{c3} on the Sc number, i.e. diffusivities, is presented in Figure 4.6. The physico-chemical properties for the different components used to calculate the dimensionless numbers are given in Table 4.3. The values of $c2$ were found to be $1.28{\cdot}10^{-2}$ and $3.80{\cdot}10^{-3}$ and the values of $c4$ were found to be 0.517 and 0.705 for the respective liquid levels of 0.121 m and 0.140 m. These values are for the specific type of reactor used in the current work, and are within the range previously reported for similar type of reactors. [88, 89] It can be clearly seen that Equation (4.2) relates the mass transfer coefficients for desorption to the same extent as for absorption. Overall it can be concluded that the empirically determined desorption mass transfer parameters can be applied to theoretical models such as the well-known film theory, penetration theory, the surface renewal theory, etc., in the same manner as absorption mass transfer parameters since the theoretical models do not differentiate between the direction of the migrating compound.

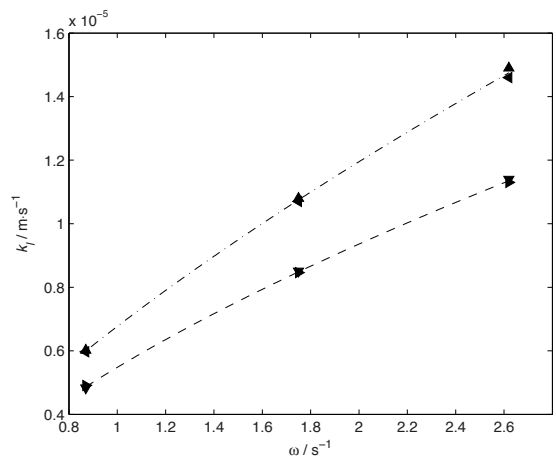

Figure 4.5: Experimental results of the influence of the stirrer speed on the mass transfer coefficients of the system carbon dioxide - water at 298.15 K: ▲, absorption at $h = 0.121$ m; ▼, absorption at $h = 0.140$ m; ◀, desorption at $h = 0.121$ m; ▶, desorption at $h = 0.140$ m; $-\cdot-\cdot-\cdot-$, Equation (4.11) at $h = 0.121$ m; $---$, Equation (4.11) at $h = 0.140$ m.

Table 4.3: Physico-chemical properties [55, 90, 92–96]

	ρ	μ	D_{CO_2}	D_{O_2}	D_{N_2O}
	$\mathrm{kg \cdot m^{-3}}$	$10^{-3}\mathrm{Pa \cdot s}$	$10^{-9}\mathrm{m^2 \cdot s^{-1}}$		
water at 298.15 K	997.00	0.890	1.93	2.00	
water at 313.15 K	992.18	0.653	2.71		
2M aq. MDEA	1018.3	1.97			1.09
2M aq. DIPA	1014.0	3.21			0.862

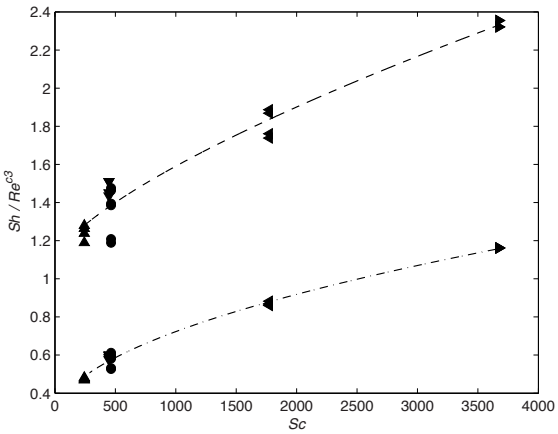

Figure 4.6: Empirical correlation of the overall results: •, carbon dioxide - water at $T = 298.15$ K; ▲, carbon dioxide - water at $T = 313.15$ K; ▼, oxygen - water at $T = 298.15$ K; ◀, nitrous oxide - 2M aq. MDEA at $T = 298.15$ K; ▶, nitrous oxide - 2M aq. DIPA at $T = 298.15$ K; $- \cdot - \cdot -$, Equation (4.12) at $h = 0.121$ m; $- - -$, Equation (4.12) at $h = 0.140$ m.

4.4 Conclusion

The liquid phase mass transfer coefficients have been measured for absorption and desorption processes. At identical operating conditions, the mass transfer coefficients for absorption and desorption appear to be the same within the reported experimental uncertainty. The desorption mass transfer coefficients depend, in the same manner as the absorption mass transfer coefficients, on the physico-chemical and the dynamic properties of the system, and can thus be related by the Sherwood, Reynolds, and Schmidt numbers. Desorption mass transfer process can further be described by the well-known film theory, penetration theory, the surface renewal theory, etc. in the same manner as absorption mass transfer processes.